CMLS, Cell. Mol. Life Sci. 62 (2005) 1462–1477
1420-682X/05/131462-16
DOI 10.1007/s00018-005-5015-5

CMLS Cellular and Molecular Life Sciences

Review

Molecular mechanism of actomyosin-based motility

M. A. Geeves [a], R. Fedorov [b] and D. J. Manstein [b, *]

[a] Department of Biosciences, University of Kent, Canterbury, Kent CT2 7NJ (United Kingdom)
[b] Institut für Biophysikalische Chemie, OE 4350, Medizinische Hochschule Hannover, Carl-Neuberg-Straße, Gebäude J4, 30623 Hannover (Germany), Fax: +49 511 532 5966, e-mail: manstein@bpc.mh-hannover.de

Received 12 January 2005; received after revision 4 March 2005; accepted 23 March 2005
Online First 28 May 2005

Abstract. Sophisticated molecular genetic, biochemical and biophysical studies have been used to probe the molecular mechanism of actomyosin-based motility. Recent solution measurements, high-resolution structures of recombinant myosin motor domains, and lower resolution structures of the complex formed by filamentous actin and the myosin motor domain provide detailed insights into the mechanism of chemomechanical coupling in the actomyosin system. They show how small conformational changes are amplified by a lever-arm mechanism to a working stroke of several nanometres, explain the mechanism that governs the directionality of actin-based movement, and reveal a communication pathway between the nucleotide binding pocket and the actin-binding region that explains the reciprocal relationship between actin and nucleotide affinity. Here we focus on the interacting elements in the actomyosin system and the communication pathways in the myosin motor domain that respond to actin binding.

Key words. Enzyme catalysis; chemomechanical coupling; protein docking; β-sheet distortion; kinetic mechanism; motor protein.

Introduction

Muscle contraction, cytoplasmic streaming in plants, amoeboid movement, cytokinesis and other types of myosin-dependent movement are driven by the cyclical interaction between the actin filament and myosin. Essential features of the actomyosin ATPase reaction were deduced from transient kinetic studies using actin filaments and myosin motor domain fragments in solution and by comparing the results with those obtained from mechanical, optical and structural measurements on rate processes in intact muscle fibres [1–5]. These studies visualized the conserved myosin motor domain as the active partner in the interaction with filamentous actin (F-actin) and established that myosin is a product-inhibited ATPase that is strongly stimulated by actin [6–8]. In the process, the 'sliding filament model' was refined to the 'swinging cross-bridge' model and, with the help of molecular engineering, single molecule approaches, and X-ray crystallography to the currently accepted 'swinging lever-arm model' [9–14]. The swinging lever-arm model predicts that the motor domain binds to actin with almost constant geometry and that small actin- and nucleotide-dependent conformational changes within the motor domain are amplified at its distal end by the extended and rigid lever-arm domain (fig. 1). The model is supported by the fact that reverse-direction movement of myosins can be achieved simply by rotating the direction of the lever arm 180° [15]. Each of the events outlined in figure 1 is a complex process that involves not only changes in the bound ligands and overall conformation of the motor domain but also local conformational changes and domain movements.

This review describes recent advances in recombinant protein production, and kinetic and structural approaches that have been applied to study the actomyosin system

* Corresponding author.

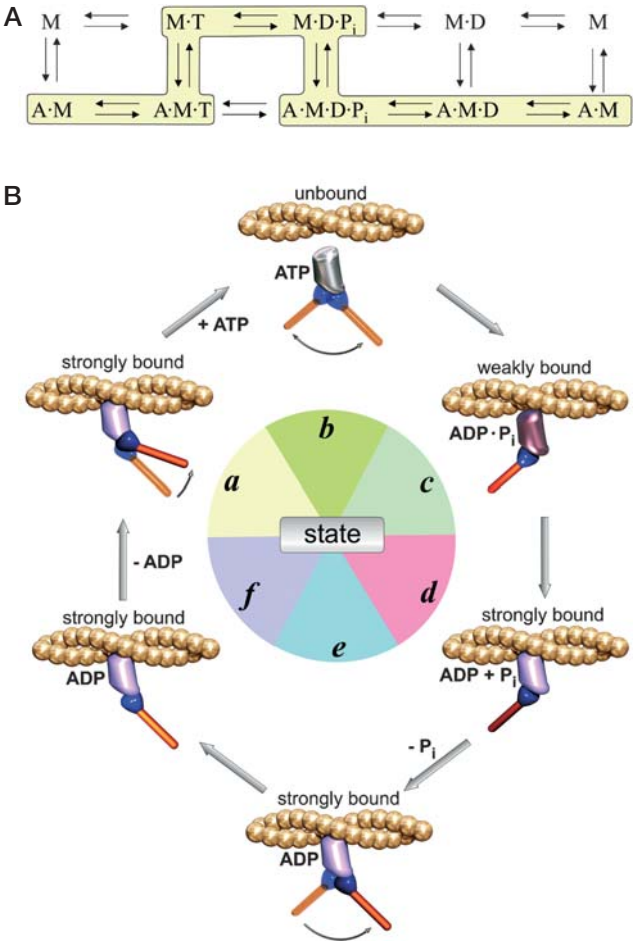

Figure 1. The actomyosin ATPase cycle. (*A*) A minimal description of the myosin and actomyosin ATPase as defined in solution. The top line represents the myosin ATPase with the following events: ATP binding, ATP hydrolysis followed by P_i release and then ADP release. The equivalent steps for actomyosin are shown in the bottom line. Vertical arrows indicate the actin association and dissociation from each myosin complex. In every case, the events shown can be broken down into a series of substeps involving one or more identifiable protein conformational changes. The states with a shaded background represent the predominant pathway for the actomyosin ATPase. (*B*) A minimal mechanochemical scheme for the actomyosin cross-bridge cycle. Starting from the rigor complex, A·M (state *a*), ATP binds to rapidly dissociate the complex and the lever arm is reprimed to the pre-power-stroke position (state *b*). This is followed by hydrolysis. The preceding three states have been well defined by crystallography, electron microscopy and solution kinetics. The exact sequence of biochemical, structural and mechanical events is more speculative. The $M{\cdot}D{\cdot}P_i$ complex rebinds to actin, initially weakly (state *c*) and then strongly (state *d*). Binding to actin induces the dissociation of P_i and the power stroke (state *e*). The completion of the tail swing (state *f*) is followed by ADP release to return to the rigor-like complex (state *a*); in some myosins (e.g. smooth-muscle myosin-II, myo1b or myosin-V) ADP dissociation is associated with a further displacement of the lever arm. Actin monomers are shown as golden spheres. The motor domain is coloured metallic grey for the free form, purple for the weakly-bound form and violet for the strongly bound form. The converter is shown in blue and the lever arm in orange.

and that have led to new insights about the mechanism of chemomechanical coupling.

Molecular genetic manipulation and expression of mutant actin and myosin constructs

Recent progress in understanding actomyosin-dependent chemomechanical transduction is to a large extent related to the production of recombinant myosin motor domains. In contrast to microtubule-based motors such as kinesin, functional myosin motors has not been produced in bacteria. Sufficient quantities of active motor domain containing myosin fragments for biochemical and structural studies have been produced only in *Dictyostelium* and the baculovirus system [16–19]. *Dictyostelium* is generally a very powerful system for the functional analysis of sequenced genes [20]. For example, most of the molecular genetic techniques typically associated with *Saccharomyces cerevisiae* are available in *Dictyostelium*, and the cells are easy to grow, lyse and process for a multitude of biochemical assays or subcellular fractionations. Studies of cytokinesis, motility, phagocytosis, chemotaxis, signal transduction and aspects of development have been greatly facilitated by the ease with which *Dictyostelium* can be manipulated by molecular genetic, biochemical and cell biological techniques [21, 22]. The high level of exogenous protein expression obtained in transformed *Dictyostelium* cells facilitates protein production and purification. Mutant versions of myosins belonging to class I, II, VII and XI have been produced in biochemical quantities in this system [23–26]. *Dictyostelium* myosin null cells can be used for the production of full-length myosins and complementation experiments with mutant myosins in this system [27]. To facilitate protein purification, vectors for the production of glutathione-S-transferase (GST) fusion proteins and His_8-, Strep-, YL1/2, and FLAG-affinity-tagged proteins were generated [28–30]. The major limitation of the *Dictyostelium* system is that high synthesis levels have been achieved reliably only with *Dictyostelium* myosins or myosin fragments. However, progress in the production of heterologous proteins in *Dictyostelium* appears likely, as the production of *Chara corallina* myosin-XI motor domain constructs, which support the movement of actin filaments in an in vitro motility assay at velocities of up to 16.2 $\mu m\ s^{-1}$, was achieved in this organism [25]. The baculovirus expression system has been successfully used to produce a wide range of myosin motors from different species including truncated isoforms of class I, II, V, VI, IX, X and XI myosins [31–35]. Although the baculovirus expression system appears to be more versatile than the *Dictyostelium* system, the production and purification of some myosin isoforms, e.g. β-cardiac myosin, have not been achieved.

His- or FLAG-tagged constructs are generally used to facilitate the purification of motor domain fragments and

subfragment-1 (S1)- or heavy meromyosin (HMM)-like constructs. Tagging of myosin constructs at either the N- or C-terminus is widely used to facilitate purification and has negligible effects on the kinetic behaviour and motor activity of the constructs [36, 37]. However, the tags can compromise the usefulness of the constructs for some applications. In single-molecule applications, tagged myosin motors appear to have a greater tendency to form clusters on the assay surface, and His-tagged myosin motors have a strong bundling effect on actin filaments.

As with to myosin, the production and purification of recombinant actin in sufficient quantities for biochemical studies is not possible in bacteria. Filament-forming distant actin homologues, such as MreB and ParM, have been identified in bacteria [38]. However, these proteins do not support myosin motor activity. In the case of actin, it has been shown that correct folding requires the eukaryotic chaperones chaperonin-containing TCP-1 (CCT) and prefoldin [39]. Sufficient quantities of mutant actins for biochemical studies have been produced in *Dictyostelium, Drosophila melanogaster, S. cerevisiae* and the baculovirus expression system [40–43]. Tagging of actin has been used to facilitate purification, but it can interfere with protein functionality. N-terminal tags tend to interfere with myosin binding, while C-terminal tags affect filament formation [44]. The baculovirus expression system appears to be the system of choice for large-scale actin expression, since more than 1 mg of untagged wild-type and mutant actin can be produced and purified from a 100-ml culture or 4×10^8 cells [45].

Structural background

Actin

Actin sequences are more highly conserved than almost any other protein. The amino-acid sequence of human skeletal muscle is 87% identical to that of yeast actin. This high degree of conservation is most likely related to the large number of proteins that specifically bind to actin. More than 50 actin-binding proteins have been characterized, and most of these proteins have been found in lower and higher eukaryotes [46–48]. Crystal structures have been obtained only with monomeric actin or G-actin (42 kDa). They show the actin monomer to consist of two similar domains, each of which contains a large and a small subdomain [49–53]. The large subdomains 2 and 3 consist of a 5-stranded β-sheet and associated α-helices (fig. 2A). The phosphate moiety of a nucleotide (ATP or ADP), together with Mg^{2+}, is bound between the two β-sheet regions. Subdomain 1 contains the DNase-binding loop, and subdomain 4 is involved in actin-actin interactions.

Homogenous and stable oligomers of filamentous actin (F-actin) for crystallographic studies were generated by cross-linking F-actin with 1,4-N,N′-phenylened maleimide and depolymerization with excess segment-1 of gelsolin (GS-1). The resulting GS-1-complexed actin trimer consists of one molecule of GS-1 bound to each actin monomer in the 178-kDa trimer complex. However, in comparison to F-actin, both the arrangement of the promoters and the intersubunit contacts responsible for stability of the actin filament are perturbed by GS-1 intercalating between the actin subunits in the mini-filament [54]. A model describing F-actin as a helical polymer was generated based on fitting the crystal structure of monomeric actin into X-ray fibre diffraction data from oriented actin gels [51]. Because the fibre diffraction patterns are of limited resolution (6–8 Å), the refinement is underdetermined and produces related but different solutions. All models show F-actin to be a helical polymer with 13 actin molecules arranged on six left-handed turns repeating every 360 Å. The rise per subunit is 27.5 Å. As the rotation per monomer is 166°, the actin helix morphology can also be described as two steep, intertwined right-handed helices (fig. 2B) [55].

It is now widely accepted that actin-based processes, which do not involve the action of a myosin motor, are required for cell locomotion and organelle movement. The formation of cellular protrusions such as lamellipodia e.g. is driven by the spatially controlled polymerization of actin in response to signalling [56–58]. Furthermore, actin filament conformational changes have been implicated in actomyosin-based motility and in regulation of motility. It is likely that binding of a myosin motor domain to actin and generation of a few pN of force will result in structural changes to actin. However, except for the elastic deformation of the filament, the form that such structural changes would take and the role they would play remain undefined. Structural changes in actin will be an area of interest in the near future, but here we concentrate on the role of the myosin motor.

Myosin motor domain

The motor fragment of myosin-II, also referred to as subfragment-1 or S1, has a tadpole-like form and consists of a central seven-stranded β-sheet and surrounding α-helices [59]. A C-terminal extension, which forms an extended α-helix and binds the two calmodulin-like ‘light chains’, is thought to act as a lever arm that amplifies small conformational changes emerging from the active site approximately 10-fold [9, 10, 14]. The proteolytic fragments of S1 are usually referred to as 25K (N-terminal), 50K and 20K (C-terminal). The central 50K fragment actually spans two structural domains, which are called the 50K upper domain (U50) and the 50K lower domain (L50) (fig. 3A). A large cleft that extends from the ATP binding site to the actin-binding region separates them. The L50 fragment (residues 465–590; unless otherwise stated sequence numbering refers to the *Dictyostelium* myosin-II heavy chain) forms a well-defined

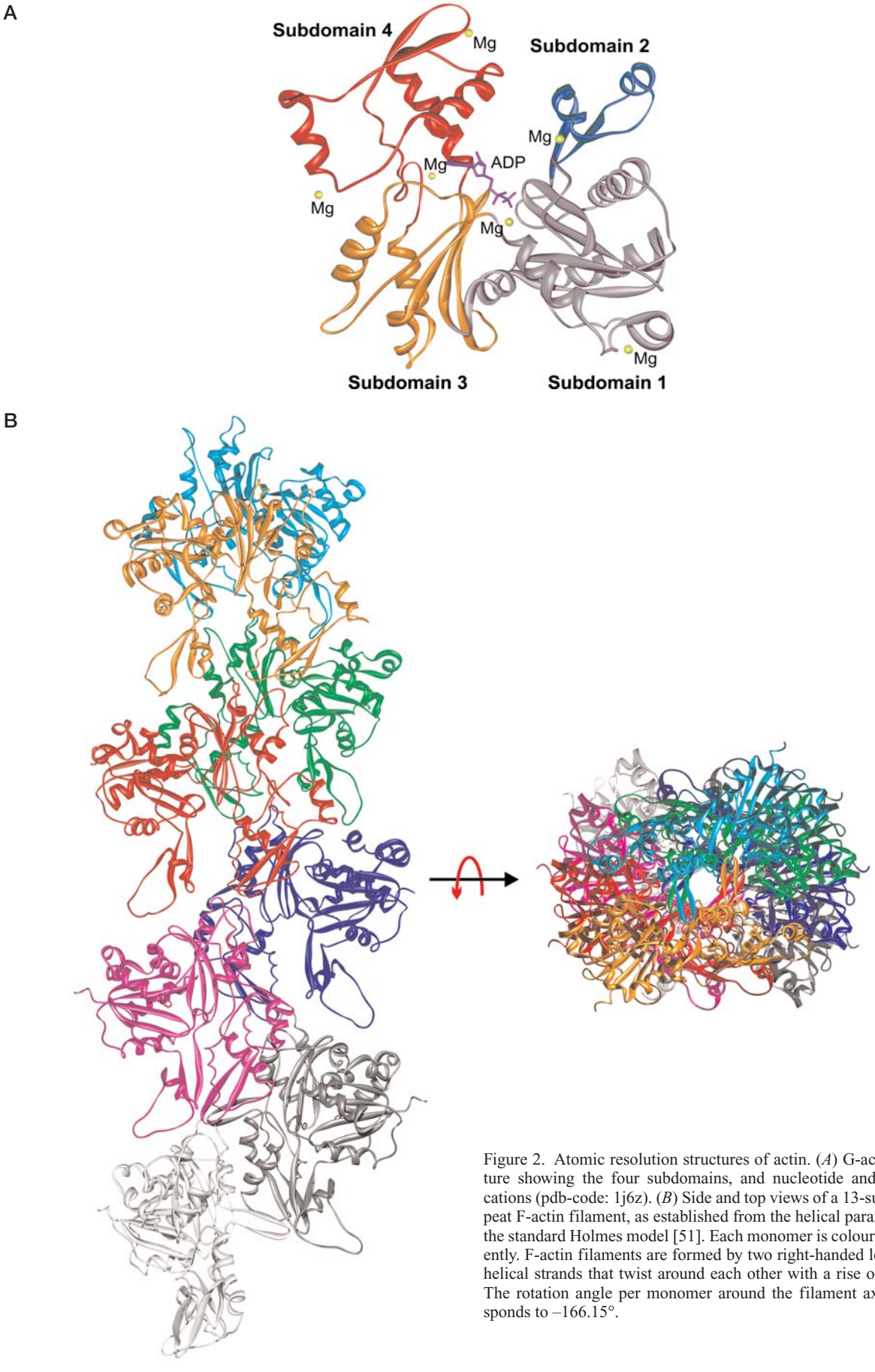

Figure 2. Atomic resolution structures of actin. (*A*) G-actin structure showing the four subdomains, and nucleotide and divalent cations (pdb-code: 1j6z). (*B*) Side and top views of a 13-subunit repeat F-actin filament, as established from the helical parameters of the standard Holmes model [51]. Each monomer is coloured differently. F-actin filaments are formed by two right-handed long pitch helical strands that twist around each other with a rise of 27.5 Å. The rotation angle per monomer around the filament axis corresponds to –166.15°.

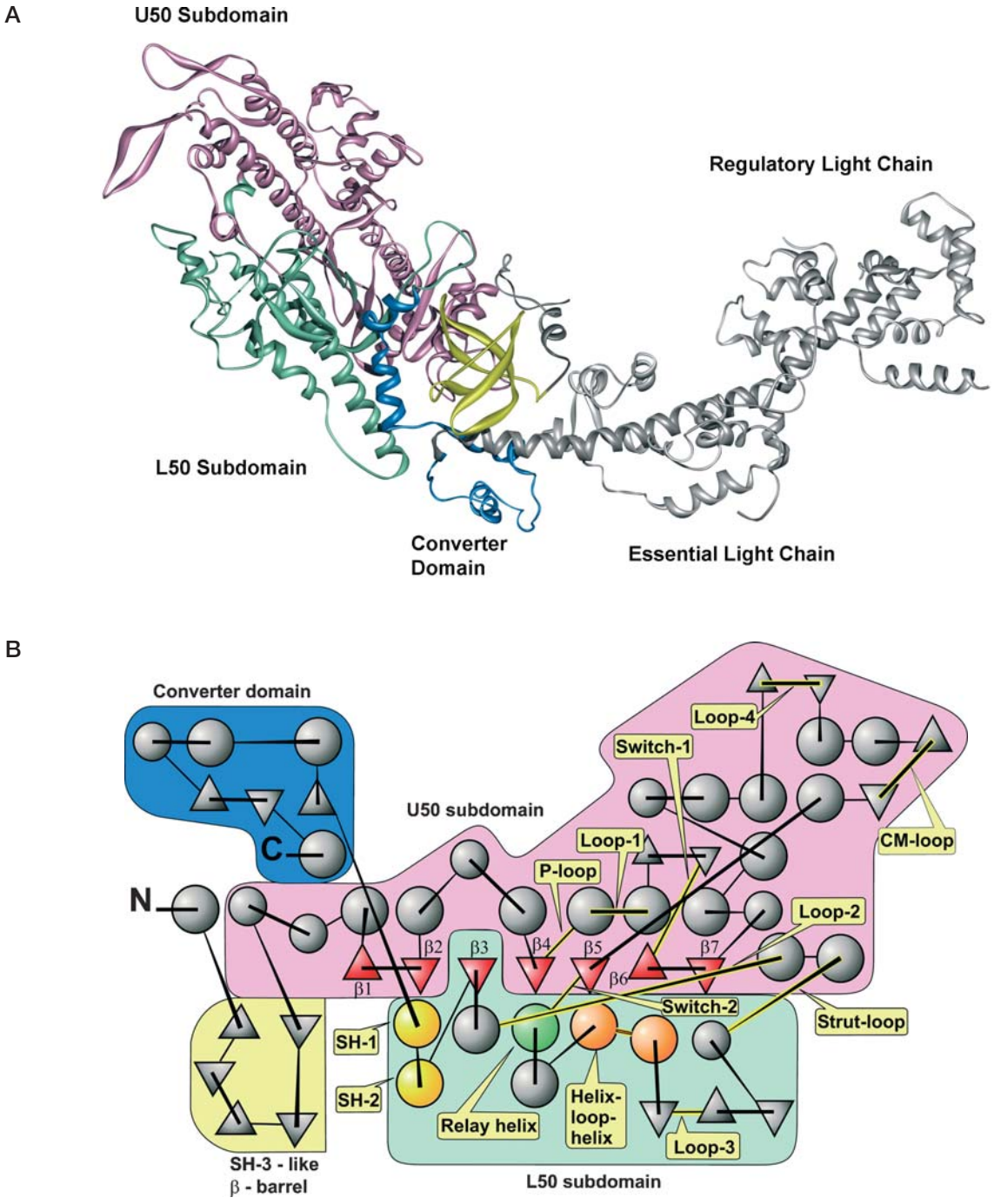

Figure 3. Structure of subfragment-1 (S1, pdb-code: 2mys) and topological map of the myosin motor domain. (*A*) S1 consists of the myosin motor domain and the light-chain-binding region, which functions as a lever arm. Colour coding for the motor domain is the same as in panel B. The light-chain- binding region of the myosin heavy chain and essential and regulatory light chains are shown in grey. (*B*) Topological map of the myosin motor domain. In addition to the domains and subdomains shown, crystallographic results reveal that the segment between β7 and switch-2 moves as a solid body and can be regarded as an independent subdomain. The SH1 and SH2 helices rotate when the β-sheet twists, which forms part of the mechanism for relieving the strain on the kinked relay helix and for driving the power stroke. Helices are shown as circles and β-strands as triangles. The background colours are N-terminal SH3-like β-barrel, yellow; U50 subdomain, pink; L50 subdomain, cyan; converter domain, light-blue. The seven-stranded central β-sheet is shown in red (β1, 116–119; β2, 122–126; β3, 649–656; β4, 173–178; β5, 448–454; β6, 240–247; β7, 253–261).

structural domain that constitutes the major part of the actin-binding site. Therefore, it is occasionally referred to as actin-binding domain. The N-terminus lies near the start of the lever arm, with residues 30–80 forming a protruding SH3-like β-barrel domain of unknown function. The rest of the 25K fragment, together with the U50 subdomain (residues 81–454 and 594–629), forms one large structural domain that accounts for six of the seven strands of the central β-sheet (fig. 3B). The actin-binding region and the nucleotide-binding site of myosin are on opposite sides of this seven-stranded β-sheet and are separated by 40–50 Å. A P-loop and two switch motifs are located in this large domain and form part of the ATP-binding site (fig. 3B). Switch-1 and switch-2 contact the nucleotide at the rear of the nucleotide-binding pocket and act as γ-phosphate sensors. The switch motifs move towards each other when ATP is bound and move away from each other when ADP occupies the binding pocket (fig. 4B). Conformational changes during this transition mostly correspond to rigid-body rotations of secondary and tertiary structure elements [59–61]. Therefore, the core and its extensions can be regarded as communicating functional units with substantial movement occurring in only a few residues.

The first part of the 20K fragment (630–670) is an integral part of the 25K – 50K domain and consists of a long helix running from the actin-binding region to the 5th strand of the central β-sheet (fig. 3B). This is followed by a turn and a broken helix. Both segments of the broken helix contain a reactive thiol in most myosins and are therefore frequently referred to as the SH1-SH2 helix. In *Dictyostelium* myosin-II, one of the conserved cysteine residues is replaced by a threonine (Thr688). A small compact domain (700–760) follows, which has been termed the 'converter' domain [60]. The converter domain functions as a socket for the C-terminal light-chain-binding domain and plays a key role in communication between the active site and the light-chain-binding domain. The light-chain-binding domain is also referred to as the 'neck' or 'lever-arm domain'.

Actomyosin interaction

Atomic models of the actomyosin complex were obtained by fitting the atomic structures of the globular myosin motor domain and F-actin into three-dimensional cryo-electron microscope reconstructions of 'decorated actin' [14, 62, 63]. In decorated actin, which is produced by incubating F-actin with motor domain fragments in the absence of nucleotide, one myosin motor domain binds to each actin monomer (fig. 4A). The models show the motor domain to form a primary contact with subdomain 1 of one actin monomer. In addition, model building brings L50 into the proximity of subdomain 2 of the next actin molecule below. The main contribution to this secondary binding site comes from loop 3 [62, 64]. The actual actin-binding region of myosin consists of a number of structures and loops including loop 3 and the helix-loop-helix motif of the L50 subdomain, the cardiomyopathy (CM) loop and loop 4 of the U50 subdomain, and loop 2 linking L50 and U50 (fig. 4A).

The helix-loop-helix motif has a similar structure in myosins from class I, II and V [59, 61, 65]. A notable feature of the helix-loop-helix motif is the presence of a number of hydrophobic residues flanked by potentially complementary ionic and polar groups.

Loop 2, which, based on sequence comparisons, appears to have completely different conformations in different myosins, has been shown to be involved in both weak and strong binding interactions with actin. It can also play an important role in controlling the rate of product release [66, 67]. Loop 3, which is located at the lower end of the actin-binding domain, contains positively charged residues and is involved in electrostatic interactions with F-actin [64]. Loop 4 does not appear to make contact with actin in atomic models of the complex between F-actin and myosin-II. However, many unconventional myosins have an extended loop-4 with a high density of charged amino acids, which may play a role in stabilizing the complex [61].

The CM loop lies at the front of the motor domain and is important for normal myosin activity. It was shown that a point mutation at position Arg403 in human β-cardiac myosin (equivalent to Arg397 in *Dictyostelium* myosin-II) is associated with familial hypertrophic cardiomyopathy [68]. The CM loop is of special interest became it contains a serine or threonine at the TEDS-site position of various unconventional myosins that plays an important role in their regulation [69–72]. Phosphorylation of this serine or threonine residue by members of the p21-activated kinase family of protein kinases (PAKs) stimulates actin-activated ATPase and motor activity [73, 74]. PAKs become activated by interaction with lipids and the GTP-bound forms of Rac and Cdc42, leading to reduced inhibition of the catalytic domain by the regulatory domain [75]. In myosin-II, aspartic or glutamic acid residues are found at the equivalent position. Motors without a negative charge at this position display low ATPase and motility [76, 77]. In the high-resolution structure of the unphosphorylated myosin IE motor domain, the CM loop is disordered, and the TEDS site is not visible. Because the CM loop is well defined in most structures of myosin motor domains, its disorder in the myosin IE structure suggests that phosphorylation may be required to constrain its orientation [78].

The total area of contact between F-actin and myosin-II corresponds to approximately 2000 Å^2. Structural and functional studies have shown a remarkable conservation in the way in which actin and myosin isoforms from different species interact. The three-dimensional atomic models of F-actin decorated with *Dictyostelium* S1 and F-actin decorated with rabbit chymotryptic S1 are very

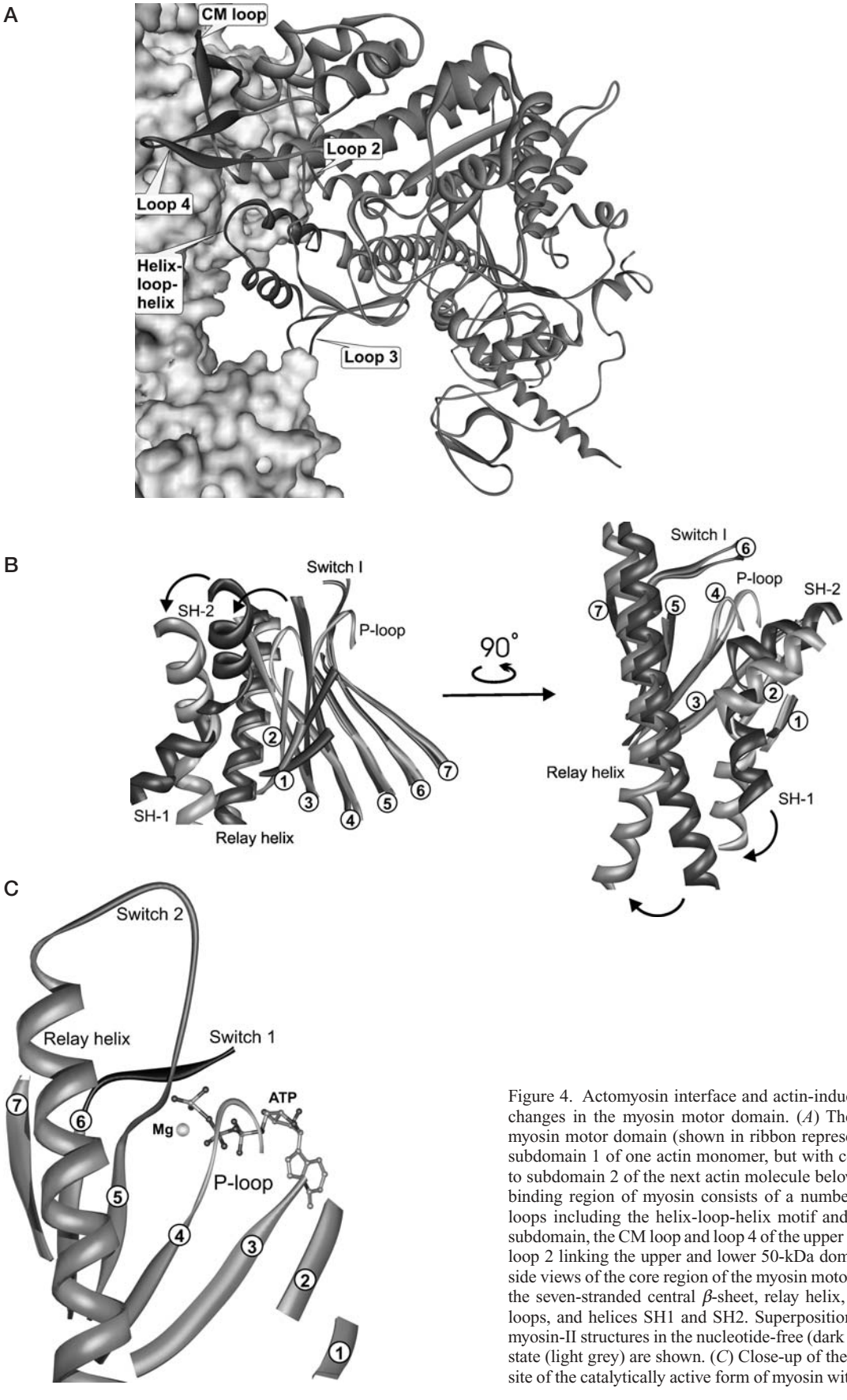

Figure 4. Actomyosin interface and actin-induced conformational changes in the myosin motor domain. (*A*) The models show the myosin motor domain (shown in ribbon representation) to bind to subdomain 1 of one actin monomer, but with considerable contact to subdomain 2 of the next actin molecule below. The actual actin-binding region of myosin consists of a number of structures and loops including the helix-loop-helix motif and loop 3 of the L50 subdomain, the CM loop and loop 4 of the upper 50-kDa domain and loop 2 linking the upper and lower 50-kDa domains. (*B*) Front and side views of the core region of the myosin motor domain, including the seven-stranded central β-sheet, relay helix, nucleotide binding loops, and helices SH1 and SH2. Superpositions of *Dictyostelium* myosin-II structures in the nucleotide-free (dark grey) and transition state (light grey) are shown. (*C*) Close-up of the nucleotide-binding site of the catalytically active form of myosin with bound Mg^{2+}-ATP.

similar, suggesting a constancy in structure of the actomyosin complex and in the details of the molecular contacts at the actomyosin interface. In regard to function, every heterologous mixture of actin and myosin tested so far shows productive interaction [25, 79]. For instance, *Dictyostelium* actin and rabbit skeletal-muscle actin move at about 2 μm s^{-1} along *Dictyostelium* myosin, and both forms of actin move at about 5 μm s^{-1} along rabbit skeletal-muscle myosin [80]. Therefore, it seems reasonable to assume that the basic mechanism of the docking process with actin is similar for myosins from different organisms and classes.

Coupling between actin- and nucleotide-binding sites

The main structural change that is apparent from computer-based fitting of myosin motor domain and actin crystal structures into the three-dimensional reconstructions of acto-S1 obtained by electron cryomicroscopy is a closing of the large cleft between the L50 and U50 subdomains [63, 81, 82]. Additional evidence that closing of the large cleft coincides with strong binding of the myosin motor domain to actin is provided by spectroscopic studies [83, 84]. Detailed structural effects of cleft closure can be deduced from the crystal structures of nucleotide-free myosin-II and myosin-V constructs [24, 65]. Large changes in the relative position of the U50 and L50 subdomains upon cleft closure in these structures lead to a distortion of the central β-sheet and, in particular, the orientation of the three edge β-strands: β1, β2 and β3. In addition, the switch-1-loop preceding β6, the switch-2-loop following β5 and the P-loop following β4 undergo large conformational changes between the nucleotide-free and the catalytically competent structures (fig. 4C). Changes in the actin interface are thereby coupled to significant movements of nucleotide-binding loop structures. Their movements result in a major disruption of interactions that stabilize γ-phosphate binding and coordination of the Mg^{2+} ion and, therefore, ADP binding. The loss of Mg^{2+}-ion coordination induced by actin binding is similar to the effect of GTPase exchange factors on the release of GDP by small G-proteins. Therefore, actin can be viewed as an ADP-exchange factor for myosin [85]. The combined effects of loss of Mg^{2+}-coordination and 'opening' of the nucleotide-binding loops explains the 10,000-fold reduction in ATP affinity. In a cell, ATP is present at millimolar concentration, which enables efficient progression in the cycle.

Binding of ATP via interactions with the P-loop as well as through ionic interactions with a positive charge provided by the unpaired arginine of the disrupted salt-bridge between switch-1 and switch-2 serves to 'close' the nucleotide-binding site in order to more fully coordinate the γ-phosphate [24, 86, 87]. This explains why ATP, but not ADP, can induce these changes. ATP-induced changes are again communicated via the strands of the central β-sheet to the U50 subdomain and lead to opening of the large cleft. Cleft opening disrupts the tight actin interface and leads to a 10,000-fold reduction in actin affinity. This sequence of events explains the reciprocal relationship between actin and nucleotide affinity. Additionally, movement of the three edge β-strands, β1, β2 and β3, is tightly coupled to that of the SH1/SH2 helices, and thereby to the relay helix (fig. 4B). A further and more direct route of communication between the converter and the L50 subdomain is linked to the movement of the relay helix as switch-2 opens and closes [11]. It appears that hydrophobic interactions and steric clashes brought about by concomitant rearrangements of β1-β3 cause the relay helix to unwind and kink when, in the presence of γ-phosphate, switch-2 is pulled up and into the nucleotide-binding site. Because the converter domain is directly adjacent to the C-terminal end of the relay helix, this bending results in a large rotation of the converter domain and, ultimately, to the swinging of the lever arm.

The interactions between the relay helix/relay loop and the converter domain occur primarily in the area between the tip of the relay loop and the converter domain and are stabilized by a number of hydrophobic residues that are among the most highly conserved residues in all classes of myosins [60]. Relay-loop residues Y494 and I499 interact with residues F692 and F745 from the converter domain. This core interaction is further supported by hydrophobic interactions involving conserved residues Y699 and I744. There are also a number of salt-bridge interactions between the completely conserved residues E490 and E493 of the relay helix and R695 and K743 of the converter.

The rearrangements following ATP binding at the nucleotide-binding site restore the catalytic competence of myosin (fig. 4C). The ensuing hydrolysis of ATP allows progression through the ATPase cycle (fig. 1). The inherent unidirectionality of the cycle is brought about by the irreversibility of the ATP-binding step. In contrast, the equilibrium dissociation constant for the hydrolysis step is close to unity. The kinetics of the product release steps determine the populations of strong and weak actin-bound states. Fast skeletal myosin-II spends approximately 5% of the cycle time in strongly bound states and is therefore sometimes referred to as a low duty ratio motor. High duty ratio motors, such as myosin-V and myosin-VI, predominantly populate the ADP-bound states (fig. 1, states *d–f*) at physiological nucleotide concentrations. Therefore, these myosins are better adapted for maintaining tension, and they have the potential to be processive [33, 77].

Biochemical kinetics and optical probes

The major molecular events in the myosin ATPase mechanism have been well described since the mid-1970s and

$$\underset{1}{M + T} \rightleftarrows \underset{2}{M \cdot T} \rightleftarrows \underset{3a}{M^{\#} \cdot T} \rightleftarrows \underset{3b}{M^{*} \cdot T} \rightleftarrows \underset{4}{M^{*} \cdot D \cdot P_i} \rightleftarrows \underset{5}{M^{\#} \cdot D \cdot P_i} \rightleftarrows \underset{6}{M^{\#} \cdot D} \rightleftarrows \underset{7}{M \cdot D} \rightleftarrows M + D$$

Scheme 1

the mechanism is most commonly referred to as the seven-step Bagshaw-Trentham scheme (scheme 1) [4].

In this mechanism, each ligand binding/dissociation event is described as a two-step process. The initial formation of a complex by diffusional collision is followed by at least one induced conformational change in the structure to give the properly docked complex. In reverse, this is an isomerization of the complex, which is required before diffusive dissociation occurs. As shown in scheme 1, the seven steps comprise two-step association of ATP, hydrolysis of ATP to leave ADP and P_i tightly bound to the protein and then two-step P_i release followed by two-step ADP release. This seven-step scheme has remained essentially unchanged since it was proposed in the mid-1970s. Each ligand binding/dissociation event may well be a more complex process, since the binding results in several local changes in structure to give the final stable structure, but in most cases it approximates to a two-step process. The original evidence for each of these events came from monitoring local structural changes from the fluorescence of intrinsic tryptophan residues [88] and nucleotide analogues [89] and from monitoring the chemical step using quenched flow methods (to follow the ATP cleavage event as well as cold chase methods to monitor tight irreversible binding of ATP) [90, 91]. Isotope exchange methods further probed details of the events [92].

More recently, the ability to express modified versions of myosin has made it possible to place tryptophan and green fluorescent protein (GFP)-type probes at different places on the molecule. This approach has been used in smooth-muscle myosin S1 and in *Dictyostelium* cytoplasmic myosin-II [13, 84, 93, 94]. These studies have clarified which parts of the molecule are involved in each of the isomerizations; the results from the different probes are summarized in table 1. These more detailed probes have not required a significant change in the description of events (except for the one listed below) but have provided a more detailed picture of which parts of myosin are involved in conformational changes.

One additional event has been added to the mechanism. Step 3 has now been shown to consist of two processes: a specific conformational change to bring the catalytic residues into the correct position to attack the β-γ ATP bond, followed by the cleavage step itself. This was predicted from crystal structures of analogues of the myosin ATP complex, which had switch-2 open; therefore, the catalytic groups were not in a position to promote hydrolysis [87]. Subsequently, it was shown that switch-2 closure preceded hydrolysis [95]. The use of single tryptophan probes and high-time resolution relaxation methods (temperature and pressure jump) allowed this change to be demonstrated [95, 96]. Values for the rates and equilibrium constants for *Dictyostelium* myosin-II are given in table 1.

Kinetics of actin binding

The low-resolution structural views of actin binding to myosin suggest that no major rearrangement of the myosin takes place at the actin-myosin interface, but that large-scale changes occur on myosin distal to the actin-binding site. However, fitting the crystal structures of myosin motor domains into three-dimensional recon-

Table 1. The rate and equilibrium constants for the Bagshaw-Trentham seven-step mechanism of the myosin ATPase with addition of step 3a/b after Holmes and Geeves [119] and Malnasi-Csizmadia et al. [123].

Step (i)	1	2	3a	3b	4	5	6	7
k_{+i}	$\geq 10^7\ M^{-1}\ s^{-1}$	$>800\ s^{-1}$	$350\ s^{-1}$	$100\ s^{-1}$	$0.05\ s^{-1}$	$\geq 10^4\ s^{-1}$	$15\ s^{-1}$	$\geq 10^4\ s^{-1}$
k_{-i}	$\geq 10^4\ s^{-1}$	$10^{-6}\ s^{-1}$	$870\ s^{-1}$	$6\ s^{-1}$	$0.003\ s^{-1}$	$\geq 10^7\ M^{-1}\ s^{-1}$	$>400\ s^{-1}$	$\geq 10^7\ M^{-1}\ s^{-1}$
K_i	$10^3\ M^{-1}$	4×10^8	79	13	15	10^3	<0.037	10^{-3} M
Signals in *Dictyostelium* myosin-II		Mant-N F239W, F242W, F129W D113W R131W	W 501 GFP/YFP-FRET	chemistry	W501 GFP/YFP-FRET chemistry		Mant-N F239W, F242W, F129W D113W R131W	

Rate and equilibrium constants are those for the *Dictyostelium* myosin-II head fragment [36, 123, 124]. FRET, fluorescence resonance energy transfer; GFP, green fluorescent protein; Mant-N, nucleotides labelled with the mant group on the 2′ or 3′ ribose hydroxyl; the one-letter code for amino acids is used.

structions obtained by electron cryomicroscopy requires closure of the large 50K cleft to form the full actomyosin interface [63, 82]. In the interaction of any two proteins, docking is likely to involve initial diffusion-limited complex formation followed by a series of structural adjustments (induced fit) as the stereospecific interaction site is formed, along with induced conformational changes in the proteins [97]. Kinetically, docking of myosin onto an actin filament can be resolved into at least three events [98] (see scheme 2). Initial complex formation, largely involving charge-charge interactions, is followed by two changes in conformation of the complex. The first may involve the formation of stereospecific hydrophobic interactions; the second involves a major rearrangement of the actin-S1 complex, since fluorescence probes on both actin and the nucleotide in the myosin pocket report the change simultaneously. The second isomerization appears to involve a large volume increase of the complex that is normally assigned to displacement of a large amount of water from the complex [67].

The three events appear similar, albeit with marked changes in rate and equilibrium constants, when they occur in the absence or presence of ADP. It has been suggested that M·ADP·P_i binds in the same three steps but that the equilibrium constant for the last step is small (~1, weak binding to actin) until P_i is displaced from the myosin [5]. The last of the conformational changes has been suggested to be closely coupled to the power stroke of the ATPase cycle [5].

In terms of the structures, we can speculate that step 0 involves long-range ionic interactions, since it is very salt dependent [67], and that step 1 is the formation of a sterospecific weak binding complex involving hydrophobic interactions, since it is not strongly affected by ionic strength but can be disrupted by the presence of organic solvent. It could therefore be the formation of the contact at the L50 subdomain. Step 2 could be the step associated with closure of the large cleft and formation of the full actomyosin-binding site, including the U50 subdomain.

The key feature of this mechanism is that the isomerization in step 2 results in a major strengthening of the actin binding to myosin and, simultaneously, a weakening of the nucleotide binding to actin [98–100], which is compatible with the structural rearrangements observed for the nucleotide-binding site of nucleotide-free myosin motor domain structures [24, 65]. As described above and shown in figure 4B, actin-induced closure of the large cleft leads to a distortion of the three edge β-strands of the central β-sheet and the nucleotide binding loops attached to β4, β5 and β6 (fig. 4C). The combined movements disrupt switch-2/P-loop interactions that stabilize γ-phosphate binding and coordination of the Mg^{2+} ion, and, thereby, ADP binding. ADP release is further facilitated by the movement of switch-1 away from the P-loop. The equilibrium constant of this step varies for different nucleotides. Thus, in the absence of nucleotide, K_2 is large (>100), while in the presence of ATP it is small ($K_2 \ll 1$) and ATP displaces actin. For other nucleotides and nucleotide analogues, K_2 is intermediate. Which form predominates, the ternary complex or the binary complex with either nucleotide or actin, depends upon the concentrations used and the lifetime of the ATP complex.

$$\mathbf{A + M} \overset{K_0}{\rightleftharpoons} \underset{\text{Collision complex}}{\mathbf{A{\sim}M}} \overset{K_1}{\rightleftharpoons} \underset{\text{A-State}}{\mathbf{A{-}M}} \overset{K_2}{\rightleftharpoons} \underset{\text{R-State}}{\mathbf{A{\cdot}M}}$$

Scheme 2

In fast rabbit myosin, formation of the R-state reduces the affinity of the myosin head for ADP more than 100-fold, and the rate of ADP dissociation is accelerated more than 500-fold. In *Dictyostelium* myosin-II, the affinity of the myosin head for ADP is reduced approximately 100-fold. In general, these factors vary more widely for different myosin types. In chicken smooth-muscle myosin, e.g. ADP affinity is reduced only 5-fold, while the dissociation rate is accelerated 10-fold by actin. Actin also induces acceleration of P_i dissociation, typically more than 200-fold. Measurement of all rate and equilibrium constants for the interaction between actin and myosin requires an extensive series of measurements. Studies of different myosins, chimaeric myosins or myosins bearing mutations have normally concentrated on a few key measurements, such as the affinity of actin for myosin in the absence of nucleotide [$K_A = K_0K_1(1 + K_2)$] and the related rate constants of association ($k_{+A} = K_0k_{+1}$) and dissociation [$k_{-A} = k_{-1}/(1 + K_2)$], or the affinity of actin for myosin in the presence of ATP at very low ionic strength (K_0 or K_0K_1, since K_2 is assumed to be negligibly small, and K_1 is undefined at low ionic strength; see Furch et al. [101]).

Mutational studies

CM loop

The CM loop is located at the distal end of the U50K subdomain (see figs 3, 4A). Involvement of this β-turn-β structure in the actin-myosin interaction has been implied by two findings. First, mutation R403Q in human β-cardiac myosin (R397Q in *Dictyostelium* myosin-II) is the cause of familial hypertrophic cardiomyopathy [68]. Experiments with a recombinant R403Q mutant, produced by baculovirus-driven co-expression of myosin heavy and light chains, showed that the protein has normal ATPase activity in the absence of actin. However, in the presence of actin, ATPase activity was more than 3-fold reduced, the K_{app} for actin binding was more than 3-fold increased and motility was 5-fold reduced. In humans, the resulting decrease in power output per unit area of cardiac muscle

is likely to provide the stimulus for hypertrophy [17]. Studies with the corresponding R397Q mutation in *Dictyostelium* myosin-II produced similar results [102].

A cluster of hydrophobic residues in the CM loop plays a role in maintaining the strong binding state. Sutoh and co-workers examined the functional importance of this region by replacing residues 398–405 (ILAGRDLV) of the *Dictyostelium* myosin-II heavy chain with the dipeptide AG. Cells producing only the mutant myosin displayed the same phenotypic defects as myosin-II null cells. They failed to grow in suspension and could not form fruiting bodies and viable spores when starved. Since partial deletion of the CM loop did not affect interaction of the mutant protein with nucleotide, as examined by steady-state and transient kinetics [103], any structural defects induced by the mutation appear to be confined to the actin-myosin interface. Therefore, the observed phenotypic changes appear to be a direct consequence of local disruption of the actin-myosin interface.

Helix-loop-helix motif

The helix-loop-helix motif includes residues S510– K546 in *Dictyostelium* myosin-II and appears to contribute to a stereospecific interaction with actin. The region has a similar structure in myosins from different classes [24, 65, 78]. A notable feature of this site is the presence of a number of hydrophobic residues flanked by potentially complementary ionic and polar groups. The effects of charge changes at positions 530–532 in this region resemble changes in the phosphorylation status of the TEDS site. The presence or absence of a single negative charge appears to play a central role in defining the affinity of the myosin head for actin and in stabilizing the A-state in particular. Giese and Spudich identified E531Q in *Dictyostelium* myosin-II as a mutation with reduced actin activation of the myosin ATPase and reduced motility [104]. In *D. discoideum* myosin-II, E531 is positioned between D530 and Q532, while in most myosins the equivalent residue is flanked by two acidic residues. The presence of negative charge at positions 531 and 532 has a major effect on actin affinity, as measured by both $\mathbf{K_A}$ (primarily $\mathbf{k_{-A}}$) and $k_{cat}/K_{M(actin)}$ [primarily $K_{M(actin)}$], with little of the change in properties being communicated to the nucleotide binding pocket. This is consistent with a two-state depiction of the myosin nucleotide pocket (strongly or weakly bound nucleotide, corresponding to the A- and R-states of scheme 2), and the charge changes affect only the concentration of actin required to induce the A-to-R-state structural change [101].

Loop 2

Loop 2 has been the focus of the majority of mutagenic studies addressing the interaction of myosin with actin. This increased interest has been due to a number of factors, including the straightforward approaches that can be taken to replace the disordered loop structure with other sequences in mutagenic studies. The myosin head is remarkably insensitive to changes in the structure of loop 2. Lengthening of the loop without concomitant charge changes produces no measurable effect on the myosin or actomyosin ATPase, the rate of ATP binding or the rate or equilibrium constants of association between actin and myosin motor. The effects of changes in the loop 2 region on the thermal stability of the myosin motor domain are in most instances small. Insertions with up to 11 uncharged amino acid residues lead to a decrease of only 1.8 °C in the thermal stability of the constructs [105]. Replacement of the native loop of smooth-muscle HMM with that from either skeletal or β-cardiac myosin caused the chimaeric HMMs to become unregulated, like the myosin from which the loop was derived, without affecting the affinity of HMM for actin in the presence of Mg.ATP or k_{cat}, the maximum turnover rate in the presence of actin [106]. Chimaeras composed of the *Dictyostelium* myosin-II backbone and of loop-2 regions from myosins of other species showed actin-activated ATPase activities that correlated well with the activity of the myosins from which the loop sequences were derived [107]. Further studies showed that the initial weak binding of myosin to actin is an electrostatic interaction between positively charged lysine residues in loop 2 and negatively charged residues in subdomain 1 of actin [64, 66, 101, 105, 108–111]. Removal of the negative charge from subdomain 1 of actin decreases the affinity of actin for myosin in the presence of Mg. ATP, while relocation of the charge in this subdomain does not alter actomyosin function, consistent with limited stereospecificity of the weak binding interaction [110, 112].

Consistent with the idea that loop 2 is a critical part of the actomyosin interface throughout the ATPase cycle, deletion of two invariant lysines at the C-terminal portion of loop 2 (K622/K623 in *Dictyostelium* myosin-II and K652/K653 in smooth muscle myosin-II) abolishes motility and actin-activated ATPase activity [66, 113]. Analysis of 11 *Dictyostelium* myosin-II mutant constructs revealed a clear correlation between charge of the loop, actin activation of the ATPase rates of the mutant constructs, and strength of the interaction between mutant motor domains and actin. The K_d for actin binding and the $K_{M(actin)}$ is decreased 10- to 120-fold when loop 2 contains 4–12 extra lysines. In the case of affinity for a nucleotide-free head, this is due to an increase in the association rate constant (k_{on}) by a factor of 5–8 and a decrease in the dissociation rate constant (k_{off}) by a factor of 5–15, suggesting that the charge on loop 2 plays a role in both formation and stabilization of the actomyosin complex. Modulation of k_{cat} by loop 2 changes has been observed for myosins with a large coupling ratio $\mathbf{K_{AD}}/K_{D,}$ showing a large reduction in affinity

for ADP upon binding to actin. The approximately 3-fold increase in k_{cat} when loop 2 contains four or more extra lysines is small in energetic terms but shows clearly that changes in loop 2 can affect the interaction of nucleotide with some myosins [67, 101]. Myosins with a small coupling ratio, such as smooth-muscle myosin-II and myosin-V do not show any increase in k_{cat} [109].

From the atomic structure of the *Dictyostelium* myosin motor domain, it appears that a minimal size of loop 2 may be required to retain correct communication between the actin- and nucleotide-binding sites [24]. Shortening of the loop is expected to produce conformational stress and a slight distortion of the myosin motor domain. The effect of loop 2 shortening on myosin motor activity was examined using a *Dictyostelium* myosin-II that had nine amino acids of this loop exchanged for a single valine residue [114]. The deletion in loop 2 did not affect the interaction with nucleotide. However, it had a large effect on the association and dissociation constants for actin binding, resulting in approximately 100-fold lower affinity for actin. Despite this large reduction in affinity, actin binding weakened the affinity of ADP for the motor approximately 60-fold, which is similar to the coupling between actin binding and ADP release observed in wild-type constructs. In contrast, the basal ATPase activity of the mutant construct is elevated 3-fold, and actin binding does not enhance ATPase activity to the normal extent. These results confirm that loop 2 is involved in high-affinity actin binding and plays a role in setting the rate of ATP hydrolysis.

Loop 3

Three-dimensional reconstructions of electron microscopy images and solution experiments performed on the actomyosin complex have suggested that loop 3, in addition to loop 2, is involved in electrostatic contacts with F-actin [14, 62–64, 115]. Because the model building brings loop 3 into the proximity of the neighbouring actin monomer, one actin helix turn below the primary site of actomyosin interaction, it is also referred to as the secondary actin-binding site of myosin. Carbodiimide-induced cross-linking between filamentous actin and myosin loop 3 is observed only with the motor domain of skeletal-muscle myosin and not with those of smooth muscle or *D. discoideum* myosin-II. Chimaeric constructs of the *D. discoideum* myosin motor domain containing loop 3 of either human skeletal muscle or nonmuscle myosin were generated. The chimaeras were fully functional, and their actin-activated ATPase activity was not affected by the substitutions. Significant actin cross-linking to the loop 3 region was obtained only with the skeletal muscle chimaera. Further analysis showed that the cross-link occurred with actin segment 1–28 [64]. A loop 3-mediated interaction with actin occurs in striated muscle myosin isoforms but is apparently not essential for either formation of a high-affinity actin-myosin interface or modulation of actomyosin ATPase activity.

Strut

The strut loop is one of three loops that connect the U50 and L50 subdomains. The loop is strongly conserved among the myosin superfamily, and its importance in maintaining the relative disposition of the two subdomains was verified by a mutagenesis study [116]. Sasaki and co-workers varied the length of the loop by deleting D590 and inserting of an Ala residue before D590 or an Ala, Asp or Pro after D590. In all cases, motility and actin-activated ATPase were substantially reduced. However, only the deletion of D590 affected the basal ATPase, which was elevated almost 10-fold. Structural studies have shown that D590 (D570 in chicken myosin-V) experiences the largest conformational changes upon cleft closure, when the region undergoes a helix-to-loop transition [24, 65, 117, 118].

Summary and future prospects

The combination of kinetic, structural and direct functional studies has led to a widely accepted view of the events in the cross-bridge cycle, from the rigor-like A·M complex through to the pre-power-stroke $M{\cdot}ADP{\cdot}P_i$ complex (fig. 1). Although a high-resolution structure of the actomyosin interface is not yet available, the combination of crystal structures of actin and myosin, high-resolution electron micrograph images of actomyosin, and optical probe data using a range of actin and myosin mutations gives us reasonable confidence in the sites of interaction. Current efforts are continuing to isolate actin trimers or small actin oligomers of defined size that would be suitable for co-crystallization with a myosin motor domain [45, 50, 54].

What remains poorly defined in both structural and biochemical terms is the exact pathway back to the rigor complex from the $M{\cdot}ADP{\cdot}P_i$ complex [119]. Figure 1B sets out a reasonably consistent pathway, but few of these complexes have been isolated and the exact sequence of the structural events remains to be defined. The rebinding of $M{\cdot}ADP{\cdot}P_i$ to actin induces the loss of P_i, which is closely coupled to the power stroke and followed by ADP dissociation. In the presence of actin, the intermediates are very short-lived in solution or in a contracting system at low load. The presence of a significant load attached to the myosin tail slows down this pathway and probably involves longer lived A·M·D and $A{\cdot}M{\cdot}D{\cdot}P_i$ complexes, but the structural details remain ill-defined. Studies of these complexes will need multifaceted approaches that combine molecular engineering with improved optical probe

techniques to follow conformational changes and binding and product release as well as the monitoring of mechanical events using single muscle fibres, myofibrils or single-molecule mechanical measurements [15, 120–122].

Acknowledgements. We thank G. Tsiavaliaris and K. C. Holmes for discussions**.** Supported by grants from the Deutsche Forschungsgemeinschaft MA1081/5-3 and MA1082/6-1 (D.J.M.) and the Wellcome Trust 070021 (M.A.G.).

1 Goldman Y. E. (1987) Kinetics of the actomyosin ATPase in muscle fibers. Ann. Rev. Physiol. **49:** 637–654
2 Lombardi V., Piazzesi G., Ferenczi M. A., Thirlwell H., Dobbie I. and Irving M. (1995) Elastic distortion of myosin heads and repriming of the working stroke in muscle. Nature **374:** 553–555
3 Piazzesi G., Reconditi M., Linari M., Lucii L., Sun Y. B., Narayanan T. et al. (2002) Mechanism of force generation by myosin heads in skeletal muscle. Nature **415:** 659–662
4 Bagshaw C. R., Eccleston J. F., Eckstein F., Goody R. S., Gutfreund H. and Trentham D. R. (1974) The magnesium ion-dependent adenosine triphosphatase of myosin. Two-step processes of adenosine triphosphate association and adenosine diphosphate dissociation. Biochem. J. **141:** 351–364
5 Geeves M. A., Goody R. S. and Gutfreund H. (1984) Kinetics of acto-S1 interaction as a guide to a model for the crossbridge cycle. J. Muscle Res. Cell Motil. **5:** 351–361
6 Reedy M. K., Holmes K. C. and Tregear R. T. (1965) Induced changes in orientation of the cross-bridges of glycerinated insect flight muscle. Nature **207:** 1276–1280
7 Huxley H. E. (1969) The mechanism of muscular contraction. Science **164:** 1356–1365
8 Lymn R. W. and Taylor E. W. (1971) Mechanism of adenosine triphosphate hydrolysis by actomyosin. Biochemistry **10:** 4617–4624
9 Anson M., Geeves M. A., Kurzawa S. E. and Manstein, D. J. (1996) Myosin motors with artificial lever arms. EMBO J. **15:** 6069–6074
10 Uyeda T. Q., Abramson P. D. and Spudich J. A. (1996) The neck region of the myosin motor domain acts as a lever arm to generate movement. Proc. Natl. Acad. Sci. USA **93:** 4459–4464
11 Geeves M. A. and Holmes K. C. (1999) Structural mechanism of muscle contraction. Annu. Rev. Biochem. **68:** 687–728
12 Spudich J. A. (2001) The myosin swinging cross-bridge model. Nat. Rev. Mol. Cell Biol. **2:** 387–392
13 Suzuki Y., Yasunaga T., Ohkura R., Wakabayashi T. and Sutoh K. (1998) Swing of the lever arm of a myosin motor at the isomerization and phosphate-release steps. Nature **396:** 380–383
14 Rayment I., Holden H. M., Whittaker M., Yohn C. B., Lorenz M., Holmes K. C. et al. (1993) Structure of the actin-myosin complex and its implications for muscle contraction. Science **261:** 58–65
15 Tsiavaliaris G., Fujita-Becker S. and Manstein D. J. (2004) Molecular engineering of a backwards-moving myosin motor. Nature **427:** 558–561
16 Manstein D. J., Ruppel K. M. and Spudich J. A. (1989) Expression and characterization of a functional myosin head fragment in *Dictyostelium discoideum*. Science **246:** 656–658
17 Sweeney H. L., Straceski A. J., Leinwand L. A., Tikunov B. A. and Faust L. (1994) Heterologous expression of a cardiomyopathic myosin that is defective in its actin interaction. J. Biol. Chem. **269:** 1603–1605
18 Trybus K. M. (1994) Regulation of expressed truncated smooth muscle myosins. Role of the essential light chain and tail length. J. Biol. Chem. **269:** 20819–20822
19 Pato M. D., Sellers J. R., Preston Y. A., Harvey E. V. and Adelstein R. S. (1996) Baculovirus expression of chicken nonmuscle heavy meromyosin II-B. Characterization of alternatively spliced isoforms. J. Biol. Chem. **271:** 2689–2695
20 Sucgang R., Shaulsky G. and Kuspa A. (2000) Toward the functional analysis of the *Dictyostelium discoideum* genome. J. Eukaryot. Microbiol. **47:** 334–339
21 Eichinger L. and Noegel A. A. (2003) Crawling into a new era – the *Dictyostelium* genome project. EMBO J. **22:** 1941–1946
22 Kreppel L., Fey P., Gaudet P., Just E., Kibbe W. A., Chisholm R. L et al. (2004) dictyBase: a new *Dictyostelium discoideum* genome database. Nucleic Acids Res. **32:** D332–333
23 Van Dijk J. V., Lafont C., Knetsch M. L., Derancourt J., Manstein D. J., Long E. C. et al. (2004) Conformational changes in actin-myosin isoforms probed by Ni(II).Gly-Gly-His reactivity. J. Muscle Res. Cell Motil. **25:** 527–537
24 Reubold T. F., Eschenburg S., Becker A., Kull F. J. and Manstein D. J. (2003) A structural model for actin-induced nucleotide release in myosin. Nat. Struct. Biol. **10:** 826–830
25 Ito K., Kashiyama T., Shimada K., Yamaguchi A., Awata J., Hachikubo Y. et al. (2003) Recombinant motor domain constructs of *Chara corallina* myosin display fast motility and high ATPase activity. Biochem. Biophys. Res. Commun. **312:** 958–964
26 Tuxworth R. I., Weber I., Wessels D., Addicks G. C., Soll D. R., Gerisch G. et al. (2001) A role for myosin VII in dynamic cell adhesion. Curr. Biol. **11:** 318–329.
27 Egelhoff T. T., Manstein D. J. and Spudich J. A. (1990) Complementation of myosin null mutants in *Dictyostelium discoideum* by direct functional selection. Dev. Biol. **137:** 359–367
28 Manstein D. J., Schuster H. P., Morandini P. and Hunt D. M. (1995) Cloning vectors for the production of proteins in *Dictyostelium discoideum*. Gene **162:**129–134
29 Knetsch M. L., Tsiavaliaris G., Zimmermann S., Rühl U. and Manstein D. J. (2002) Expression vectors for studying cytoskeletal proteins in *Dictyostelium discoideum*. J. Muscle Res. Cell Motil. **23:** 605–611
30 Levi S., Polyakov M. and Egelhoff T. T. (2000) Green fluorescent protein and epitope tag fusion vectors for *Dictyostelium discoideum*. Plasmid **44:** 231–238
31 Homma K., Saito J., Ikebe R. and Ikebe M. (2001) Motor function and regulation of myosin X. J. Biol. Chem. **276:** 34348–34354
32 Inoue A., Saito J., Ikebe R. and Ikebe M. (2002) Myosin IXb is a single-headed minus-end-directed processive motor. Nat. Cell Biol. **4:** 302–306
33 De La Cruz E. M., Wells A. L., Rosenfeld S. S., Ostap E. M. and Sweeney H. L. (1999) The kinetic mechanism of myosin V. Proc. Natl. Acad. Sci. USA **96:** 13726–13731
34 Wells A. L., Lin A. W., Chen L. Q., Safer D., Cain S. M., Hasson T. et al. (1999) Myosin VI is an actin-based motor that moves backwards. Nature **401:** 505–508
35 Batters C., Arthur C. P., Lin A., Porter J., Geeves M. A., Milligan R. A. et al. (2004) Myo1c is designed for the adaptation response in the inner ear. EMBO J. **23:** 1433–1440
36 Kurzawa S. E., Manstein D. J. and Geeves M. A. (1997) *Dictyostelium discoideum* myosin II: characterization of functional myosin motor fragments. Biochemistry **36:** 317–323
37 Ritchie M. D., Geeves M. A., Woodward S. K. and Manstein D. J. (1993) Kinetic characterization of a cytoplasmic myosin motor domain expressed in *Dictyostelium discoideum*. Proc. Natl. Acad. Sci. USA **90:** 8619–8623
38 Lowe J., van den Ent F. and Amos L. A. (2004) Molecules of the bacterial cytoskeleton. Annu. Rev. Biophys. Biomol. Struct. **33:** 177–198
39 Rommelaere H., Van Troys M., Gao Y., Melki R., Cowan N. J., Vandekerckhove J. et al. (1993) Eukaryotic cytosolic chaperonin contains t-complex polypeptide 1 and seven related subunits. Proc. Natl. Acad. Sci. USA **90:** 11975–11979

40 Anson M., Drummond D. R., Geeves M. A., Hennessey E. S., Ritchie M. D. and Sparrow J. C. (1995) Actomyosin kinetics and in vitro motility of wild-type *Drosophila* actin and the effects of two mutations in the Act88F gene. Biophys. J. **68:** 1991–2003

41 Sutoh K., Ando M. and Toyoshima Y. Y. (1991) Site-directed mutations of *Dictyostelium* actin: disruption of a negative charge cluster at the N terminus. Proc. Natl. Acad. Sci. USA **88:** 7711–7714

42 Cook R. K., Root D., Miller C., Reisler E. and Rubenstein P. A. (1993) Enhanced stimulation of myosin subfragment 1 ATPase activity by addition of negatively charged residues to the yeast actin NH2 terminus. J. Biol. Chem. **268:** 2410–2415

43 Schuler H., Korenbaum E., Schutt C. E., Lindberg U. and Karlsson R. (1999) Mutational analysis of Ser14 and Asp157 in the nucleotide-binding site of beta-actin. Eur. J. Biochem. **265:** 210–220

44 Rommelaere H., Waterschoot D., Neirynck K., Vandekerckhove J. and Ampe C. (2004) A method for rapidly screening functionality of actin mutants and tagged actins. Biol. Proced. Online **6:** 235–249

45 Joel P. B., Fagnant P. M. and Trybus K. M. (2004) Expression of a nonpolymerizable actin mutant in Sf9 cells. Biochemistry **43:** 11554–11559

46 McCurdy D. W., Kovar D. R. and Staiger C. J. (2001) Actin and actin-binding proteins in higher plants. Protoplasma **215:** 89–104

47 Noegel A. A. and Schleicher M. (2000) The actin cytoskeleton of *Dictyostelium*: a story told by mutants. J. Cell Sci. **113 (Pt 5):** 759–766

48 Van Troys M., Vandekerckhove J. and Ampe C. (1999) Structural modules in actin-binding proteins: towards a new classification. Biochim. Biophys. Acta **1448:** 323–348

49 Otterbein, L. R., Cosio C., Graceffa P. and Dominguez R. (2002) Crystal structures of the vitamin D-binding protein and its complex with actin: structural basis of the actin-scavenger system. Proc. Natl. Acad. Sci. USA **99:** 8003–8008

50 Otterbein L. R., Graceffa P. and Dominguez R. (2001) The crystal structure of uncomplexed actin in the ADP state. Science **293:** 708–711

51 Holmes K. C., Popp D., Gebhard W. and Kabsch W. (1990) Atomic model of the actin filament. Nature **347:** 44–49

52 Schutt C. E., Myslik J. C., Rozycki M. D., Goonesekere N. C. and Lindberg U. (1993) The structure of crystalline profilin-beta-actin. Nature **365:** 810–816

53 McLaughlin P. J., Gooch J. T., Mannherz H. G. and Weeds A. G. (1993) Structure of gelsolin segment 1-actin complex and the mechanism of filament severing. Nature **364:** 685–692

54 Dawson J. F., Sablin E. P., Spudich J. A. and Fletterick R. J. (2003) Structure of an F-actin trimer disrupted by gelsolin and implications for the mechanism of severing. J. Biol. Chem. **278:** 1229–1238

55 Tirion M. M., ben-Avraham D., Lorenz M. and Holmes K. C. (1995) Normal modes as refinement parameters for the F-actin model. Biophys. J. **68:** 5–12

56 Carlier M. F., Wiesner S., Le Clainche C. and Pantaloni D. (2003) Actin-based motility as a self-organized system: mechanism and reconstitution in vitro. Crit. Rev. Biol. **326:** 161–170

57 Bernheim-Groswasser A., Wiesner S., Golsteyn R. M., Carlier M. F. and Sykes C. (2002) The dynamics of actin-based motility depend on surface parameters. Nature **417:** 308–311

58 Pantaloni D., Le Clainche C. and Carlier M. F. (2001) Mechanism of actin-based motility. Science **292:** 1502–1506

59 Rayment I., Rypniewski W. R., Schmidt-Bäse K., Smith R., Tomchick D. R., Benning M. M. et al. (1993) Three-dimensional structure of myosin subfragment-1: a molecular motor. Science **261:** 50–58

60 Dominguez R., Freyzon Y., Trybus K. M. and Cohen C. (1998) Crystal structure of a vertebrate smooth muscle myosin motor domain and its complex with the essential light chain: visualization of the pre-power stroke state. Cell **94:** 559–571

61 Kliche W., Fujita-Becker S., Kollmar M., Manstein D. J. and Kull F. J. (2001) EMBO J. **20:** 40–46

62 Schröder R. R., Manstein D. J., Jahn W., Holden H., Rayment I., Holmes K. C. et al. (1993) Three-dimensional atomic model of F-actin decorated with *Dictyostelium* myosin S1. Nature **364:** 171–174

63 Holmes K. C., Angert I., Kull F. J., Jahn W. and Schröder R. R. (2003) Electron cryo-microscopy shows how strong binding of myosin to actin releases nucleotide. Nature **425:** 423–427

64 Van Dijk J., Furch M., Lafont C., Manstein D. J. and Chaussepied P. (1999) Functional characterization of the secondary actin binding site of myosin II. Biochemistry **38:** 15078–15085

65 Coureux P. D., Wells A. L., Menetrey J., Yengo C. M., Morris C. A., Sweeney H. L. et al. (2003) A structural state of the myosin V motor without bound nucleotide. Nature **425:** 419–423

66 Van Dijk J., Furch M., Derancourt J., Batra R., Knetsch M. L., Manstein D. J. et al. (1999) Differences in the ionic interaction of actin with the motor domains of nonmuscle and muscle myosin II. Eur. J. Biochem. **260:** 672–683

67 Furch M., Geeves M. A. and Manstein D. J. (1998) Modulation of actin affinity and actomyosin adenosine triphosphatase by charge changes in the myosin motor domain. Biochemistry **37:** 6317–6326

68 Geisterfer-Lowrance A. A., Kass S., Tanigawa G., Vosberg H. P., McKenna W., Seidman C. E. et al. (1990) A molecular basis for familial hypertrophic cardiomyopathy: a beta cardiac myosin heavy chain gene missense mutation. Cell **62:** 999–1006

69 Ostap E. M., Lin T., Rosenfeld S. S. and Tang N. (2002) Mechanism of regulation of *Acanthamoeba* myosin-IC by heavy-chain phosphorylation. Biochemistry **41:** 12450–12456

70 Bement W. M. and Mooseker M. S. (1995) TEDS rule: a molecular rationale for differential regulation of myosins by phosphorylation of the heavy chain head. Cell Motil. Cytoskel. **31:** 87–92

71 Brzeska H. and Korn E. D. (1996) Regulation of class I and class II myosins by heavy chain phosphorylation. J. Biol. Chem. **271:** 16983–16986

72 Fujita-Becker S., Dürrwang U., Erent M., Clark R. J., Geeves M. A. and Manstein D. J. (2004) Changes in Mg^{2+}-ion concentration and heavy chain phosphorylation regulate the motor activity of a class-I myosin. J. Biol. Chem. **280:** 6064–6071

73 Brzeska H., Szczepanowska J., Hoey J. and Korn E. D. (1996) The catalytic domain of *Acanthamoeba* myosin I heavy chain kinase: II. Expression of active catalytic domain and sequence homology to p21-activated kinase (PAK). J. Biol. Chem. **271:** 27056–27062

74 Wu C., Lee S. F., Furmaniak-Kazmierczak E., Cote G. P., Thomas D. Y. and Leberer E. (1996) Activation of myosin-I by members of the Ste20p protein kinase family. J. Biol. Chem. **271:** 31787–31790

75 Buchwald G., Hostinova E., Rudolph M. G., Kraemer A., Sickmann A., Meyer H. E. et al. (2001) Conformational switch and role of phosphorylation in PAK activation. Mol. Cell Biol. **21:** 5179–5189

76 Wang Z. Y., Wang F., Sellers J. R., Korn E. D. and Hammer J. A. 3rd (1998) Analysis of the regulatory phosphorylation site in *Acanthamoeba* myosin IC by using site-directed mutagenesis. Proc. Natl. Acad Sci. USA **95:** 15200–15205

77 De La Cruz E. M., Ostap E. M. and Sweeney H. L. (2001) Kinetic mechanism and regulation of myosin VI. J. Biol. Chem. **276:** 32373–32381

78 Kollmar M., Dürrwang U., Kliche W., Manstein D. J. and Kull F. J. (2002) Crystal structure of the motor domain of a class-I myosin. EMBO J. **21:** 2517–2525
79 Herm-Götz A., Weiss S., Stratmann R., Fujita-Becker S., Ruff C., Meyhöfer E. et al. (2002) *Toxoplasma gondii* myosin A and its light chain: a fast, single-headed, plus-end-directed motor. EMBO J. **21:** 2149–2158
80 Kron S. J., Drubin D. G., Botstein D. and Spudich J. A. (1992) Yeast actin filaments display ATP-dependent sliding movement over surfaces coated with rabbit muscle myosin. Proc. Natl. Acad. Sci. USA **89:** 4466–4470
81 Volkmann N., Ouyang G., Trybus K. M., DeRosier D. J., Lowey S. and Hanein D. (2003) Myosin isoforms show unique conformations in the actin-bound state. Proc. Natl. Acad. Sci. USA **100:** 3227–3332
82 Volkmann N., Hanein D., Ouyang G., Trybus K. M., DeRosier D. J. and Lowey S. (2000) Evidence for cleft closure in actomyosin upon ADP release. Nat. Struct. Biol. **7:** 1147–1155
83 Conibear P. B., Bagshaw C. R., Fajer P. G., Kovacs M. and Malnasi-Csizmadia A. (2003) Myosin cleft movement and its coupling to actomyosin dissociation. Nat. Struct. Biol. **10:** 831–835
84 Yengo C. M., De La Cruz E. M., Chrin L. R., Gaffney D. P. 2nd and Berger C. L. (2002) Actin-induced closure of the actin-binding cleft of smooth muscle myosin. J. Biol. Chem. **277:** 24114–24119
85 Goody R. S. and Hofmann-Goody W. (2002) Exchange factors, effectors, GAPs and motor proteins: common thermodynamic and kinetic principles for different functions. Eur. Biophys. J. **31:** 268–274
86 Furch M., Fujita-Becker S., Geeves M. A., Holmes K. C. and Manstein D. J. (1999) Role of the salt-bridge between switch-1 and switch-2 of *Dictyostelium* myosin. J. Mol. Biol. **290:** 797–809
87 Zeng W., Conibear P. B., Dickens J. L., Cowie R. A., Wakelin S., Malnasi-Csizmadia A. et al. (2004) Dynamics of actomyosin interactions in relation to the cross-bridge cycle. Philos. Trans. R. Soc. Lond. B Biol. Sci. **359:** 1843–1855.
88 Batra R. and Manstein D. J. (1999) Functional characterisation of *Dictyostelium* myosin II with conserved tryptophanyl residue 501 mutated to tyrosine. Biol. Chem. **380:** 1017–1023
89 Woodward S. K., Eccleston J. F. and Geeves, M. A. (1991) Kinetics of the interaction of 2′(3′)-O-(N-methylanthraniloyl)-ATP with myosin subfragment 1 and actomyosin subfragment 1: characterization of two acto-S1-ADP complexes. Biochemistry **30:** 422–430
90 Biosca J. A., Barman T. E. and Travers F. (1984) Transient kinetics of the binding of ATP to actomyosin subfragment 1: evidence that the dissociation of actomyosin subfragment 1 by ATP leads to a new conformation of subfragment 1. Biochemistry **23:** 2428–2436
91 Kuhlman P. A. and Bagshaw C. R. (1998) ATPase kinetics of the *Dictyostelium discoideum* myosin II motor domain. J. Muscle Res. Cell Motil. **19:** 491–504
92 Geeves M. A., Webb M. R., Midelfort C. F. and Trentham D. R. (1980) Mechanism of adenosine 5′-triphosphate cleavage by myosin: studies with oxygen-18-labeled adenosine 5′-triphosphate. Biochemistry **19:** 4748–4754
93 Shih W. M., Gryczynski Z., Lakowicz J. R. and Spudich J. A. (2000) A FRET-based sensor reveals large ATP hydrolysis-induced conformational changes and three distinct states of the molecular motor myosin. Cell **102:** 683–694
94 Wakelin S., Conibear P. B., Woolley R. J., Floyd D. N., Bagshaw C. R., Kovacs M. et al. (2002) Engineering *Dictyostelium discoideum* myosin II for the introduction of site-specific fluorescence probes. J. Muscle Res. Cell Motil. **23:** 673–683
95 Malnasi-Csizmadia A., Pearson D. S., Kovacs M., Woolley R. J., Geeves M. A. and Bagshaw C. R. (2001) Kinetic resolution of a conformational transition and the ATP hydrolysis step using relaxation methods with a *Dictyostelium* myosin II mutant containing a single tryptophan residue. Biochemistry **40:** 12727–12737
96 Urbanke C. and Wray J. (2001) A fluorescence temperature-jump study of conformational transitions in myosin subfragment 1. Biochem. J. **358:** 165–173
97 Schreiber G. and Fersht A. R. (1996) Rapid, electrostatically assisted association of proteins. Nat. Struct. Biol. **3:** 427–431
98 Geeves M. A. and Conibear P. B. (1995) The role of three-state docking of myosin S1 with actin in force generation. Biophys. J. **68:** 194S–199S
99 Goody R. S. and Holmes K. C. (1983) Cross-bridges and the mechanism of muscle contraction. Bioch. Biophys. Acta **726:** 13–39
100 Taylor E. W. (1991) Kinetic studies on the association and dissociation of myosin subfragment 1 and actin. J. Biol. Chem. **266:** 294–302
101 Furch M., Remmel B., Geeves M. A. and Manstein D. J. (2000) Stabilization of the actomyosin complex by negative charges on myosin. Biochemistry **39:** 11602–11608
102 Fujita H., Sugiura S., Momomura S., Sugi H. and Sutoh K. (1998) Functional characterization of *Dictyostelium discoideum* mutant myosins equivalent to human familial hypertrophic cardiomyopathy. Adv. Exp. Med. Biol. **453:** 131–137
103 Sasaki N., Asukagawa H., Yasuda R., Hiratsuka T. and Sutoh K. (1999) Deletion of the myopathy loop of *Dictyostelium* myosin II and its impact on motor functions. J. Biol. Chem. **274:** 37840–37844
104 Giese K. C. and Spudich, J. A. (1997) Phenotypically selected mutations in myosin's actin binding domain demonstrate intermolecular contacts important for motor function. Biochemistry **36:** 8465–8473
105 Ponomarev M. A., Furch M., Levitsky D. I. and Manstein D. J. (2000) Charge changes in loop 2 affect the thermal unfolding of the myosin motor domain bound to F-actin. Biochemistry **39:** 4527–4532
106 Rovner A. S., Freyzon Y. and Trybus K. M. (1995) Chimeric substitutions of the actin-binding loop activate dephosphorylated but not phosphorylated smooth muscle heavy meromyosin. J. Biol. Chem. **270:** 30260–30263
107 Uyeda T. Q., Ruppel K. M. and Spudich J. A. (1994) Enzymatic activities correlate with chimaeric substitutions at the actin-binding face of myosin. Nature **368:** 567–569
108 Johara M., Toyoshima Y. Y., Ishijima A., Kojima H., Yanagida T. and Sutoh K. (1993) Charge-reversion mutagenesis of *Dictyostelium* actin to map the surface recognized by myosin during ATP-driven sliding motion. Proc. Natl. Acad. Sci. USA **90:** 2127–2131
109 Yengo C. M. and Sweeney H. L. (2004) Functional role of loop 2 in myosin V. Biochemistry **43:** 2605–2612
110 Wong W. W., Doyle T. C. and Reisler E. (1999) Nonspecific weak actomyosin interactions: relocation of charged residues in subdomain 1 of actin does not alter actomyosin function. Biochemistry **38:** 1365–1370
111 Miller C. J., Wong W. W., Bobkova E., Rubenstein P. A. and Reisler E. (1996) Mutational analysis of the role of the N terminus of actin in actomyosin interactions. Comparison with other mutant actins and implications for the cross-bridge cycle. Biochemistry **35:** 16557–16565
112 Miller C. J. and Reisler E. (1995) Role of charged amino acid pairs in subdomain-1 of actin in interactions with myosin. Biochemistry **34:** 2694–2700
113 Joel P. B., Trybus K. M. and Sweeney H. L. (2001) Two conserved lysines at the 50/20-kDa junction of myosin are necessary for triggering actin activation. J. Biol. Chem. **276:** 2998–3003
114 Knetsch M. L., Uyeda T. Q. and Manstein D. J. (1999) Disturbed communication between actin- and nucleotide-binding sites in a myosin II with truncated 50/20-kDa junction. J. Biol. Chem. **274:** 20133–20138

115 Ikebe M., Onishi H. and Tonomura Y. (1982) Difference between smooth and skeletal muscle myosins in the stoichiometry of their reactions with ATP: identical and nonidentical two-headed structures of smooth and skeletal muscle myosins. J. Biochem. (Tokyo) **91:** 1855–1873
116 Sasaki N., Ohkura R. and Sutoh K. (2000) Insertion or deletion of a single residue in the strut sequence of *Dictyostelium* myosin II abolishes strong binding to actin. J. Biol. Chem. **275:** 38705–38709
117 Holmes K. C., Schröder R. R., Sweeney H. L. and Houdusse A. (2004) The structure of the rigor complex and its implications for the power stroke. Philos. Trans. R. Soc. Lond. B Biol. Sci. **359:** 1819–1828
118 Coureux P. D., Sweeney H. L. and Houdusse A. (2004) Three myosin V structures delineate essential features of chemo-mechanical transduction. EMBO J. **23:** 4527–4537
119 Holmes K. C. and Geeves M. A. (2000) The structural basis of muscle contraction. Philos. Trans. R. Soc. Lond. Biol. Sci. **355:** 419–431
120 Webb M. R., Reid G. P., Munasinghe V. R. and Corrie J. E. (2004) A series of related nucleotide analogues that aids optimization of fluorescence signals in probing the mechanism of P-loop ATPases, such as actomyosin. Biochemistry **43:** 14463–14471
121 Brune M., Corrie J. E. and Webb M. R. (2001) A fluorescent sensor of the phosphorylation state of nucleoside diphosphate kinase and its use to monitor nucleoside diphosphate concentrations in real time. Biochemistry **40:** 5087–5094
122 Corrie J. E., Brandmeier B. D., Ferguson R. E., Trentham D. R., Kendrick-Jones J., Hopkins S. C. et al. (1999) Dynamic measurement of myosin light-chain-domain tilt and twist in muscle contraction. Nature **400:** 425–430
123 Malnasi-Csizmadia A., Woolley R. J. and Bagshaw C. R. (2000) Resolution of conformational states of *Dictyostelium* myosin II motor domain using tryptophan (W501) mutants: implications for the open-closed transition identified by crystallography. Biochemistry **39:** 16135–16146
124 Batra R., Geeves M. A. and Manstein D. J. (1999) Kinetic analysis of *Dictyostelium discoideum* myosin motor domains with glycine-to-alanine mutations in the reactive thiol region. Biochemistry **38:** 6126–6134